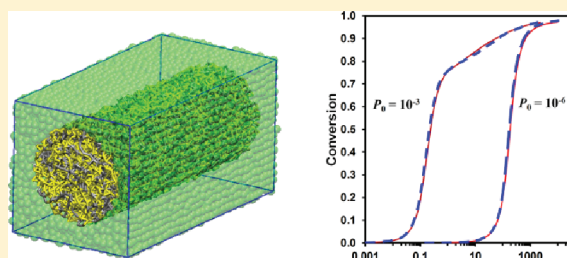


Effect of Nanoconfinement on Kinetics of Cross-Linking Reactions: A Molecular Simulation Study

Po-Han Lin,[†] Swapnil C. Kohale,[‡] and Rajesh Khare*

Department of Chemical Engineering, Texas Tech University, Lubbock, Texas 79409-3121, United States

ABSTRACT: We have used molecular dynamics simulations to study the effect of nanoconfinement on the kinetics of cross-linking reactions. Specifically, a bead–spring model is used to carry out reactive molecular dynamics simulations of the autocatalytic epoxy curing reactions. In this simple model, if two colliding molecules arrive in spatial proximity, they react to form a new bond with a specified probability. The kinetics of the reaction in the bulk was compared with that in a cylindrical pore. Our simulations show that confinement leads to an increase in both the translational mobility of the beads as well as the average displacement undergone by the beads from their initial position to the position of reaction. The net result of these opposing factors is that the rate of curing reaction in the confinement is quantitatively similar to that in the bulk. We also observed heterogeneity of reaction rates in the confined system. As compared to the reaction rate in the bulk, the reaction rate in the first layer near the pore wall is lower, whereas the reaction rate in the central core domain of the nanopore hardly shows any difference from the bulk value except in the high conversion stage. The results suggest that the reaction rate in the confined system relative to the bulk will vary with the relative volume fractions of the first layer near the wall and the central core domain.



INTRODUCTION

Ever since the early work of Jackson and McKenna,^{1,2} it is well-known that nanoscale confinement of small organic molecules and polymers affects their thermal properties such as melting point and glass transition temperature (T_g). One of the major findings of their work was that the phase transition temperature (either for the first- or second-order transition as the case may be) shifts under confinement and the shift is strongly dependent on the length scale of confinement. In the last two decades, numerous theoretical, experimental and simulation studies have examined the nanoscale confinement effects on structural, dynamic and thermal properties for a variety of confined and confining materials; these studies are summarized in several reviews.^{3–7} These studies have not shown a unifying trend of the effect of confinement. For example, T_g has been shown to increase or decrease or is unaffected under confinement.⁴

Recently, effect of nanoconfinement on reaction kinetics has also been studied. Experiments carried out by Simon and co-workers^{8–11} showed that the kinetics of cure reaction of mono- and dicyanate esters confined in controlled pore glass (CPG) is accelerated with a reduction in the pore size. Several factors that could lead to enhanced kinetics were examined including possible lowering of apparent activation energy for curing reaction and the effect of surface chemistry. Their results showed that the apparent activation energies were quantitatively similar in the bulk and the confined systems. In terms of surface chemistry, even though the hydroxyl groups on the internal surface of CPG catalyze the curing reaction, this effect was considered to be presumably eliminated by replacing the hydroxyl groups with trimethylsilyl groups (i.e., silanization). It was thus hypothesized

in their work that the acceleration of curing kinetics could be attributed to an increase in the collision frequency due to the confinement. Furthermore, Begum and Simon¹² also used kinetic modeling to study the effect of nanopore confinement on methyl methacrylate free radical polymerization. The diffusivity of poly(methyl methacrylate) chains was considered to decrease as the size of the pore decreases. They found that the gel effect (i.e., a steep increase in the rate of free radical polymerization as well as the average molecular weight) was shifted such that it occurred at shorter times and at lower conversions as the size of the nanopore became smaller.

Experimentally, it is challenging to investigate the detailed structure of polymers in nanoscale confinement as well as to explicitly account for the interfacial interactions between the confined material and the confining surface; molecular simulations provide such ability.^{13–16} Scheidler et al.^{13,14} investigated the relaxation behavior of supercooled liquids composed of binary mixture of Lennard-Jones (LJ) particles in the vicinity of smooth and rough walls. Specifically, they focused solely on the geometric effect by excluding the surface layering effect in the confined systems. Their results showed that the relaxation time of supercooled fluids increased significantly next to the rough wall, whereas it decreased in the vicinity of the smooth wall. Malvaldi et al.¹⁵ carried out molecular dynamics (MD) simulations to examine a polymer melt system confined between two parallel surfaces of LJ sites; they observed that the strong

Received: April 25, 2011

Revised: August 8, 2011

Published: October 06, 2011

attracting walls significantly increase the relaxation time of polymer melts. Vogel¹⁶ reported the rotational and conformational dynamics of poly(ethylene oxide) melt near a fixed TiO₂ surface by using an all-atom model, showing that the dynamic behavior of polymer chains in the layer close to the surface slowed down as compared to the polymer chains in the bulk.

In addition to dynamics, effect of confinement on reaction kinetics has also been studied using simulations. Specifically, stepwise bimolecular polymerization of linear polymer chains under confinement was studied by using the lattice Monte Carlo technique.¹⁷ This study showed that confinement has two competing effects on the reaction kinetics: higher density and slower diffusion. Although the former was found to increase the reaction rate, the latter reduced the reaction rate. Consequently, the net effect could be either an enhancement or suppression of the reaction kinetics depending on the interactions between the polymer chains themselves and the polymer chains and the confining wall particles.

In this work, the cure kinetics of cross-linked epoxy under nanoscale confinement was studied by MD simulations. We use a continuous off-lattice model and chain dynamics is explicitly considered in our MD simulations. We have used a coarse-grained, bead–spring model to carry out reactive MD simulations of the autocatalytic cross-linking reactions. The kinetics of the reaction in the bulk was compared with that in a cylindrical pore. In addition to the effect of confinement on the collision frequency, the effect of reaction probability on the rate of reaction was also studied. Our simulation results are discussed in the context of experimental data on the effect of nanoconfinement on the cure kinetics.

■ MOLECULAR MODEL AND SIMULATION DETAILS

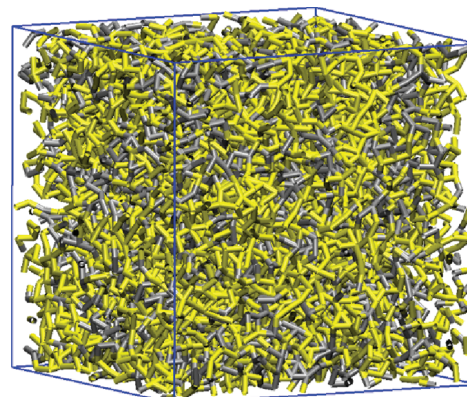
Two types of systems were studied in this work: bulk and confined systems. As shown in Figure 1, the bulk system consists of two types of molecules: epoxy monomers and cross-linkers; in addition to these two molecules, the confined system also contains the wall atoms which create a cylindrical channel. All of the atoms in these systems interact with each other via Weeks–Chandler–Andersen (WCA) potential,¹⁸ a purely repulsive Lennard-Jones (LJ) potential, given by

$$U_{\text{WCA}}(r) = \begin{cases} 4\epsilon \left[\left(\frac{\sigma}{r}\right)^{12} - \left(\frac{\sigma}{r}\right)^6 \right] + \epsilon & r < 2^{1/6}\sigma \\ 0 & r \geq 2^{1/6}\sigma \end{cases} \quad (1)$$

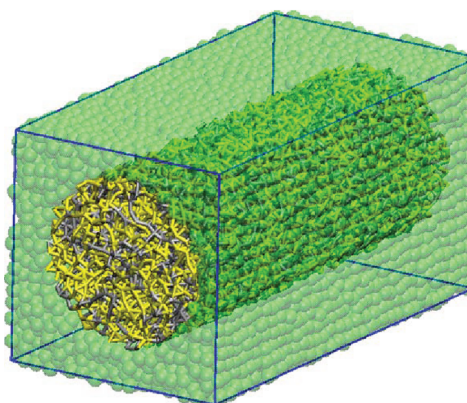
where σ is LJ diameter and ϵ is LJ potential well depth. All of the quantities in the rest of the paper are reported in the reduced LJ units. In our coarse-grained representation, the epoxy monomers and cross-linkers were modeled as dumbbells in which the beads are connected by the harmonic springs represented by the potential

$$U_{ij} = \frac{k_r}{2} (r_{ij} - r_{\text{eq}})^2 \quad (2)$$

where $k_r = 500$ and $r_{\text{eq}} = 1.1$. In bulk system, the dimension of the cubic box was 22.0 and periodic boundary conditions were applied in all the directions. In the confined system, the box dimensions were 45.5, 23.4, and 23.4 respectively in the x , y , and z directions. The model structure was confined in y and z



(a)

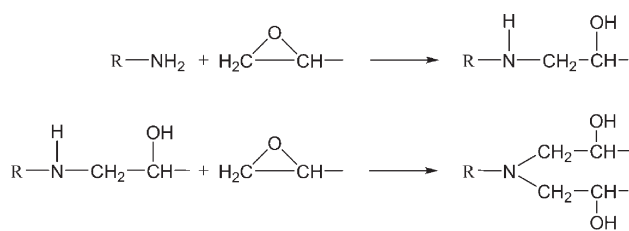


(b)

Figure 1. Model structures of (a) bulk system and (b) confined system. The epoxy, cross-linker, and the wall atoms are shown in yellow, gray, and green colors, respectively.

directions by wall atoms and thus periodic boundary conditions were applied only in the x direction. The cylindrical channel containing a pore of radius $r = 9$ was composed of the wall atoms attached to the face centered cubic (FCC) lattice sites by harmonic springs. The lattice spacing for the wall atoms was 1.3; the spring constant was 500. The latter value was chosen to prevent the confined molecules from leaking out of the walls.¹⁹

Constant NVT (constant number of atoms, constant volume, and constant temperature) MD simulations were implemented in this study. We note that the change in the density between the final cross-linked matrix and the initial mixture of epoxy monomers and cross-linkers has been found to be very small in experimental work and is considered to be negligible.²⁰ We also note that the effects of the heat of reaction are not explicitly accounted for in our model. Our model thus represents an isothermal cure process; such isothermal cure has also been reported in experimental studies.^{8,21} For the bulk system, the temperature was maintained at the specified value by coupling all the atoms to the heat bath using a velocity Verlet type algorithm for Brownian dynamics.^{19,22} In the confined system only the wall atoms were coupled to a heat bath using the same algorithm, corresponding

**Figure 2.** Schematic of the curing reaction.

to the experimental setup that the temperature of the confined materials is maintained through the confining wall. In this case, the trajectories of the beads of the confined molecules were calculated by the usual velocity Verlet algorithm for MD simulation. For all the simulations conducted in this work, a time step of 0.001 was used. The number density of both systems was chosen to be 0.84.

MECHANISM OF CROSS-LINKING REACTION AND MODELING METHOD

The specific cross-linking reaction studied here is the autocatalytic reaction between epoxy monomers and diamines, as shown in Figure 2. Such cross-linked epoxy systems have been well-studied in experiments.^{20,21,23} The curing of epoxy involves the reactions between the amino groups on diamine and the epoxide groups on the epoxy monomer. The hydroxyl groups formed during the curing reaction are found to catalyze both reactions shown in Figure 2. Based on the assumptions of equal reactivity of all amino hydrogens, presence of initial stoichiometric quantities of epoxy monomers and amines in the initial mixture, and the initial existence of the hydroxyl groups due to the presence of some impurities or a few epoxy monomers that have reacted during sample preparation, the overall reaction kinetics can be formulated as²¹

$$\frac{dx}{dt} = k(1-x)^2(x + B) \quad (3)$$

where x is the conversion of epoxy, k is the overall reaction constant and B is a constant associated with the initial concentrations of both epoxide and hydroxyl groups. The conversion x is defined as

$$x = \frac{E_{\text{reacted}}}{E_{\text{total}}} \quad (4)$$

where E_{reacted} and E_{total} are the number of reacted and total epoxide groups, respectively. For the reaction to take place, the molecules containing the potential reacting sites first diffuse within spatial proximity and then react. The rate constant for the overall process is thus given by

$$\frac{1}{k} = \frac{1}{k_{\text{rxn}}} + \frac{1}{k_{\text{diff}}} \quad (5)$$

where k_{rxn} and k_{diff} denote rate constants for the intrinsic reaction and diffusion steps, respectively. The rate constant of intrinsic reaction can be evaluated by the Arrhenius equation

$$k_{\text{rxn}} = Ae^{-\Delta E/k_B T} \quad (6)$$

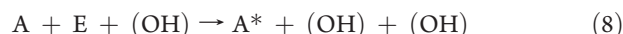
where A is a prefactor associated with collision frequency and ΔE , k_B , and T are the activation energy (i.e., energy barrier) of the reaction, Boltzmann constant, and temperature, respectively.

We can also define the reaction probability P_{rxn} in terms of the activation energy and the temperature as

$$P_{\text{rxn}} = e^{-\Delta E/k_B T} \quad (7)$$

When the activation energy approaches zero, P_{rxn} reaches a maximum value of one, implying that the reactants will immediately react when they arrive in spatial proximity.

As suggested in the literature, the rate-determining step in the curing reaction could be either a bimolecular or trimolecular reaction.²⁴ Here we consider both possibilities. In our coarse-grained representation, epoxy monomers and cross-linkers are modeled as dumbbells; each bead of the dumbbell represents a reacting site (e.g., epoxide group or amino group). For the trimolecular reaction, the autocatalytic reaction process can be expressed as



where E , A , A^* , and (OH) represent epoxide, unreacted amino, reacted amino, and hydroxyl groups, respectively. A few hydroxyl groups were initially introduced into the system by designating some epoxide groups as "reacted" beads. As expected, this setup will affect the initial concentration of the catalyst in the system as well as the constant B in eq 3, thus leading to a change in the reaction rate. Given the setup mentioned above, MD simulations were carried out at temperature $T = 1.0$ with initial conversion $x_0 = 0.002$ in the bulk and confined systems. The reaction was considered to take place by formation of new bonds when the epoxide, amino, and hydroxyl groups arrive in spatial proximity of each other. Specifically, if the distance between all three pairs [i.e., $A-E$, $E-(\text{OH})$, and $A-(\text{OH})$], during the simulation becomes less than 1.1, a random number was generated to check if a new bond can be formed. If the number thus generated is smaller than the reaction probability P_{rxn} , a new bond is created to connect these epoxide and amino groups. This procedure is repeated at each MD step.

For the bimolecular reaction case, the curing reaction is considered to consist of a sequence of bimolecular reactions with the reaction rate being determined by the reaction between the amino group and a complex consisting of epoxide and a hydrogen from a donor. In other words, the rate-determining step is a bimolecular reaction. Similar simulation method as that described for the trimolecular reaction was used for this case. The two differences were that the hydroxyl groups were not introduced into the system initially and the reaction probability P_{rxn} was considered to increase with an increase in the conversion to take into account the kinetic enhancement due to the autocatalytic reaction. P_{rxn} was considered to be linearly dependent on the conversion and was expressed by the relation:²¹

$$P_{\text{rxn}} = P_0(1 + ax) \quad (9)$$

where P_0 is the initial reaction probability and a is a positive constant. We have selected values of 10^{-3} and 10^{-6} for P_0 in our calculations. Based on the experimental data in the literature,²¹ we selected a value of 18 for the constant a . We note that our goal is to capture the essential physics and chemistry of the process and not to exactly map our coarse grained model onto the experimental system. The reaction rate was monitored by collecting data for the conversion as a function of time. The data thus collected were used to characterize the effects of confinement and reaction probability in both systems on the curing kinetics.

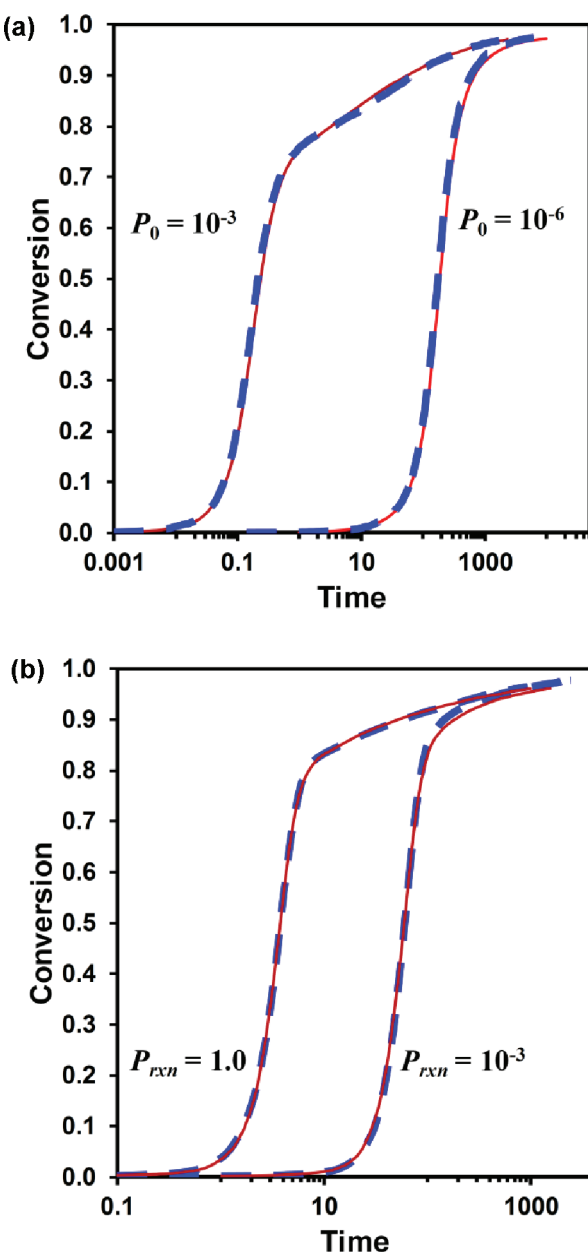


Figure 3. Reaction profile as a function of time in the bulk (dashed blue line) and the confined (solid red line) systems at $T = 1.0$. Figure shows results for (a) bimolecular reaction for initial reaction probabilities, $P_0 = 10^{-3}$ and 10^{-6} , and (b) trimolecular reaction for reaction probabilities, $P_{rxn} = 1.0$ and 10^{-3} .

RESULTS AND DISCUSSION

Effect of Confinement on the Reaction Rate. To investigate the effect of nanoscale confinement on collision frequency during the curing reaction, two separate simulations were carried out under the same conditions (i.e., same temperature, reaction probability, and initial concentration of catalyst) in the bulk and in the confined systems, respectively.

Figure 3 represents the reaction curves as a function of time in both bulk and confined systems for two different values of reaction probabilities. Results for both bimolecular and trimolecular reaction cases are shown in the figure. In all cases, the shape of the simulated conversion curves is very similar to that reported for

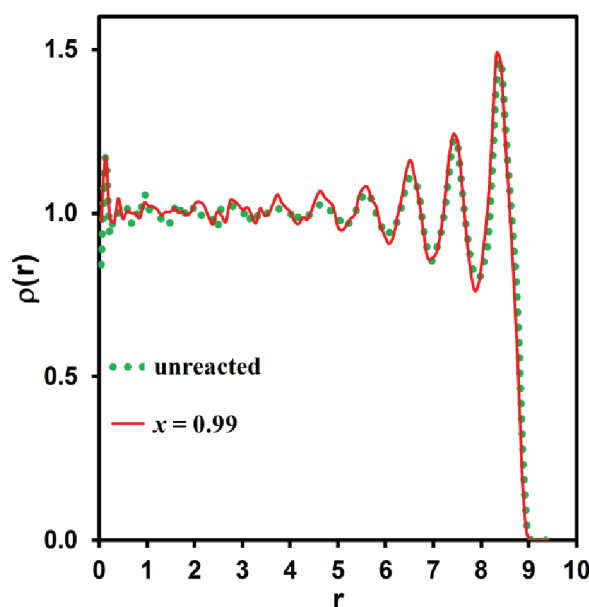


Figure 4. Density distribution function of the beads in the cylindrical pore in the initial (unreacted) and final stages of the curing reaction for $P_0 = 10^{-3}$. r denotes the radial distance from the central axis of the cylinder.

the experimental data.²¹ The epoxy curing reaction can be characterized into three stages: initiation, rapid acceleration and high conversion. Initially, the reaction rate (i.e., the slope of the curve) is very low due to the presence of a very small amount of catalyst (i.e., hydroxyl group) in the system. As epoxy monomers and cross-linkers gradually react, the reaction becomes much faster with an increase in the concentration of hydroxyl groups. Once the majority of the reactants form the cross-linked epoxy, the reaction significantly slows down due to low concentration of the reactants as well as the slowdown of diffusion of reactants owing to the growth in the network structure. Generally, the high conversion stage is considered to be diffusion-controlled, whereas the initiation and rapid acceleration stages are considered to be reaction-controlled. However, in case of the reaction probability $P_{rxn} = 1.0$, the activation energy of curing reaction equals zero, indicating that the potentially reacting pairs immediately react once they diffuse into spatial proximity, and the reaction is diffusion-controlled over the entire duration of time.

As can be seen in Figure 3, there is a very small, if at all, difference between the reaction curves in the bulk and confined systems in all three stages. A comparison of Figure 3, panels a and b, also indicates that the conversion curves are very similar for the bimolecular and trimolecular cases. Given this, we will only focus on the bimolecular case in the rest of the paper.

Molecular Packing and Reaction Rate. To further elucidate the confinement effect on the reaction rate of the beads, we focus on the detailed structure of the molecules under confinement. We observed that there is no measurable difference between the density profiles for the two sets of calculations with initial reaction probabilities $P_0 = 10^{-3}$ and 10^{-6} , thus for the sake of clarity, only one set of results (for $P_0 = 10^{-3}$) is shown in Figure 4. As can be seen in Figure 4, the beads of epoxy and cross-linkers form at least four well-defined high density layers near the pore surface with a bulk-like region of uniform density in the central region of the pore. Furthermore, the figure also shows that there is no

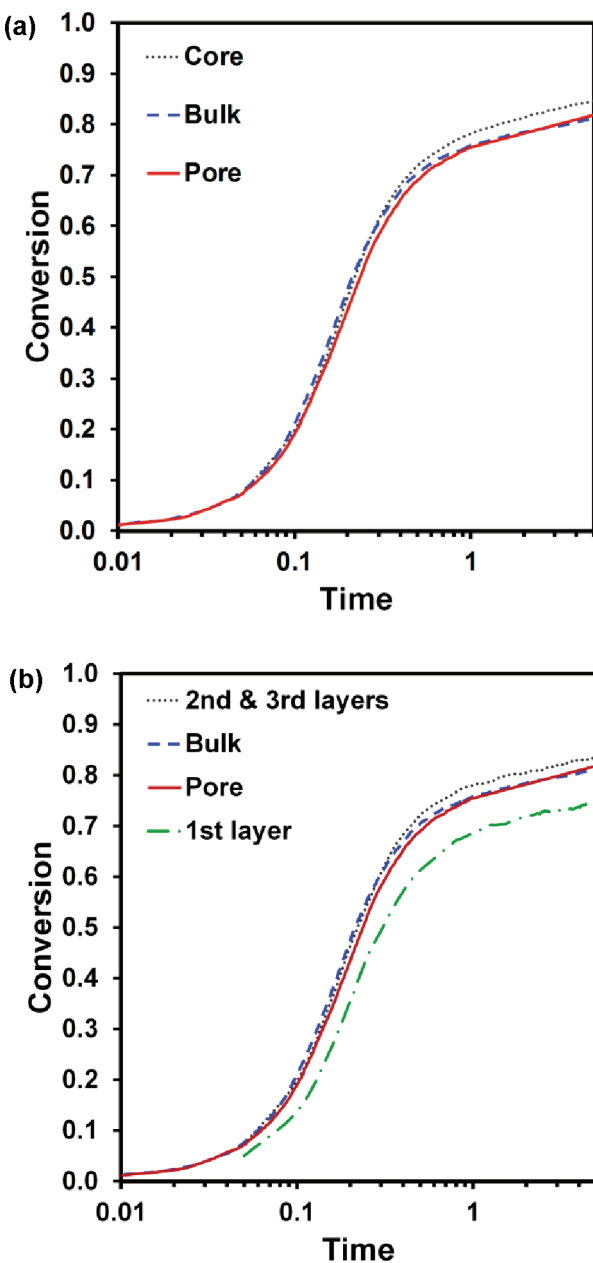


Figure 5. Comparison of the overall conversion profile in the bulk and the cylindrical pore with the conversion profiles in (a) the core region and (b) the near-wall region in the cylindrical pore at $P_0 = 10^{-3}$ and $T = 1.0$.

difference in the packing behavior in the beginning and the end stages of the cure process.

In order to determine the effect of density variation on the reaction rate, we next compared the reaction curves of the epoxy monomers and the cross-linkers in the near-wall region with those in the bulk-like core region. For this purpose, we partition the pore into three domains: an outer shell domain consisting of the first bead layer close to the wall ($8.0 \leq r < 9.0$), another shell domain consisting of the second and third bead layers near the wall ($6.0 \leq r < 8.0$), and the innermost cylindrical domain consisting of the central core region ($0.0 \leq r < 6.0$). Figure 5 shows a comparison of the reaction curves of these regions in confined systems with the bulk system for initial reaction probability $P_0 = 10^{-3}$. In Figure 5a, we find that the reaction rate in

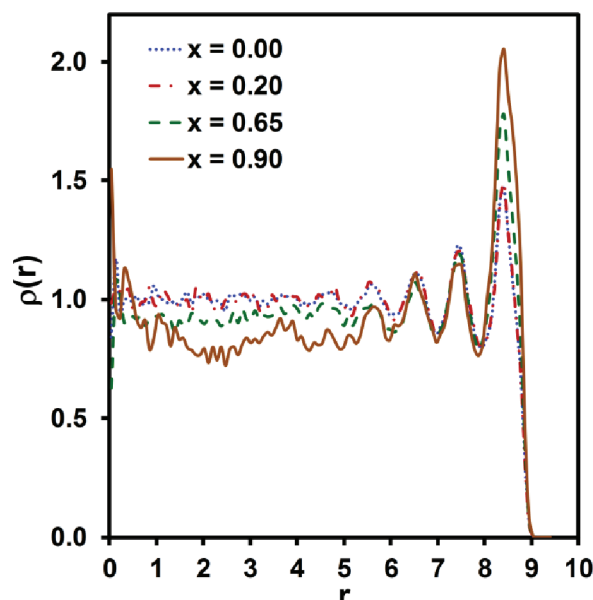


Figure 6. Density distribution function of the still-able-to-react beads in the cylindrical pore at four different conversions. r denotes the radial distance from the central axis of the cylinder.

the central core region is effectively the same as that in the bulk, except in the high conversion stage. Furthermore, we also observe in Figure 5b that the reaction rate in the shell domain consisting of the second and third layers close to the wall is almost the same as that in the central core region, whereas the reaction rate is consistently lower as compared to the bulk in the first bead layer near the wall.

In addition to the total bead density, the density distribution of the unreacted beads is also of interest. Figure 6 shows the density profile of the still-able-to-react beads which consist of all the unreacted beads of epoxy monomers and cross-linkers, and the reacted beads of cross-linkers that have formed only one bond with an epoxy monomer. The curves in Figure 6 were normalized by the number density of these beads at the specific conversion. As the conversion increases, the relative density of still-able-to-react beads within the first layer near the wall becomes higher, while the relative density of these beads in the central core region decreases. These results indicate that in the confined system, the reaction rate in the first layer near the wall is lower than that in the central core domain, which is consistent with the reaction curves shown in Figure 5.

Dynamics of Epoxy and Cross-Linkers. In addition to the detailed structure, the dynamic properties of the molecular system are also expected to be affected under nanoconfinement. We characterized the translational mobility of still-able-to-react beads at two different conversions by measuring their mean-squared displacement (MSD) as a function of time. Due to the confinement in the radial direction, the curves of the confined system shown here are for the MSD in the axial direction only. We note that the MSD in the bulk system is isotropic; for the purposes of comparison with the MSD in the nanopore, the values of MSD in the bulk were divided by 3. In the bulk system (see Figure 7), the MSD curve at 0% conversion shows free diffusive behavior for the translation of unreacted epoxy monomer and cross-linkers as indicated by the slope value of one. As the conversion increases, the overall translational mobility of

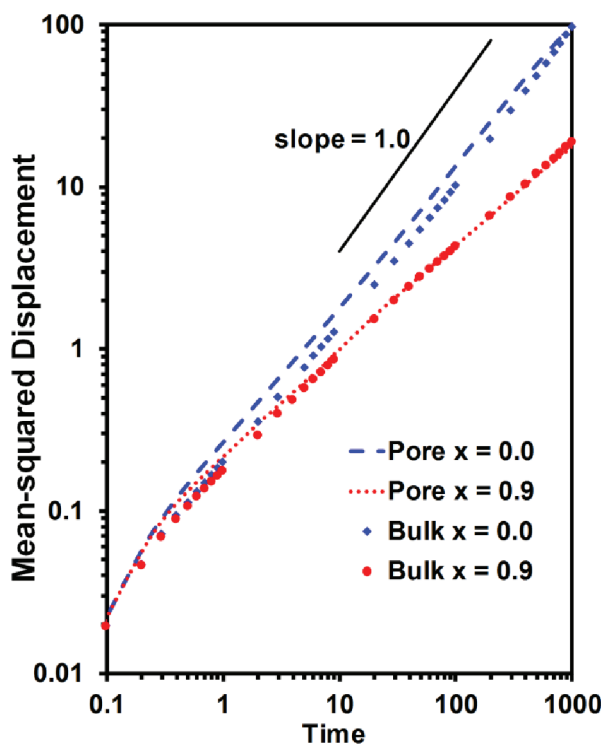


Figure 7. Mean-squared displacement (MSD) of still-able-to-react beads at two conversions in the bulk and the confined systems. MSD in only the axial direction is shown for the confined system, and the bulk values are divided by three for the sake of comparison on the plot.

still-able-to-react beads decreases and shows a subdiffusive behavior as is evident from the values of slope that are less than unity. We attribute this subdiffusive behavior to the restriction on the bead motion imposed by the cross-linked network structure; similar anomalous diffusion of small particles or biomolecules in viscoelastic media such as polymer networks^{25,26} or in confinement by a static boundary or a dynamic crowding environment^{27–30} has also been reported in the literature. As compared to the bulk system, the overall mobility of still-able-to-react beads in the confined system is slightly higher at 0% conversion but the difference begins to vanish with an increase in conversion. Similar to the bulk case, the slope of MSD curves in the confined system also decreases as the conversion increases. Moreover, we have also characterized the translational mobility of the still-able-to-react beads near the wall. Figure 8 shows the MSD curves of the still-able-to-react beads which were initially located within the first layer near the wall for a specific conversion. These beads might be able to move away from the wall; to study this possibility, the density distribution of these beads in the radial direction at four different times is shown in Figure 9. These curves are normalized by the initial total number of these beads and thus the area under each curve is unity. Our simulations show that the average MSD value of the beads that were initially located in the vicinity of the wall is lower than the average value of MSD of the still-able-to-react beads in the entire confined system over the time t less than 100, i.e., when more than half of those beads initially located near the wall are still in that region. Over a longer time scale (i.e., $t \sim 1000$), the beads that were initially located near the wall get distributed in the whole pore and thus their MSD curves merge with the MSD curves of all of the still-able-to-react beads in the confined system.

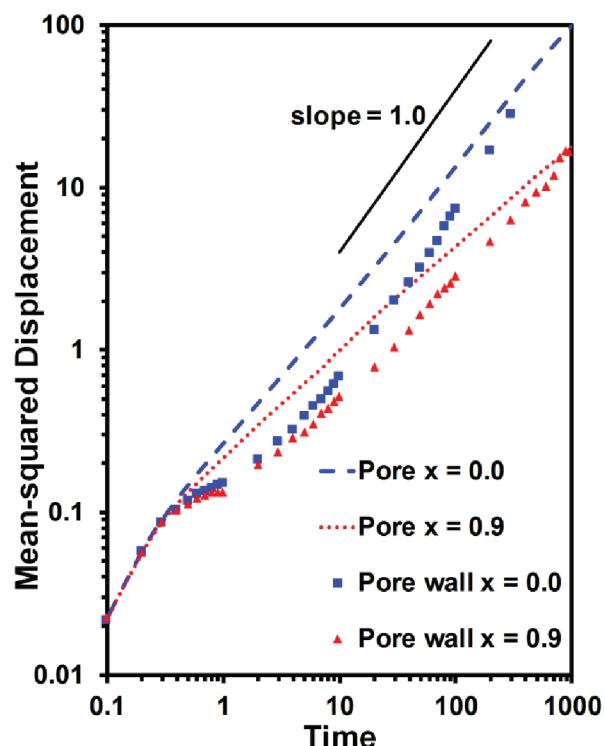


Figure 8. Mean-squared displacement (MSD) of still-able-to-react beads at two conversions in the confined system. The figure shows a comparison of the overall MSD of these beads in the pore with the MSD of these beads in the first layer near the wall.

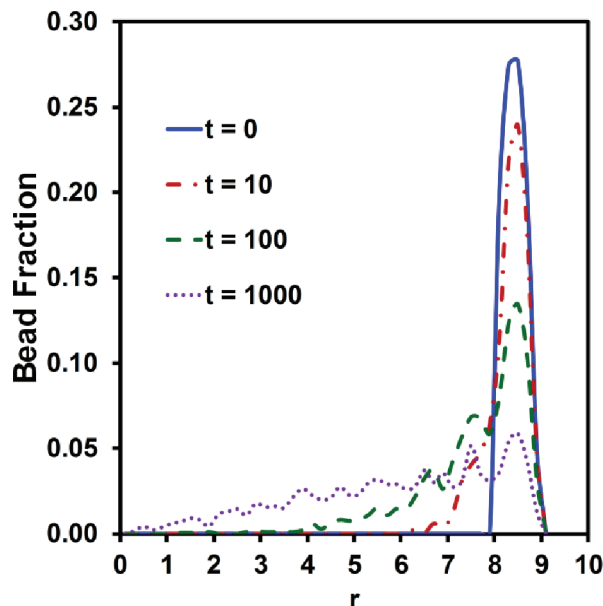


Figure 9. Density distribution of the still-able-to-react beads that were initially located in the first layer near the wall. The curves are normalized on the basis of the number of beads that were initially in the first layer.

In addition to the mobility of the molecules as determined by the MSD, another aspect of interest is the displacement undergone by an unreacted bead from its initial position to the position where it reacts. To characterize this quantity, we defined the mean reaction path as the average displacement (as opposed to

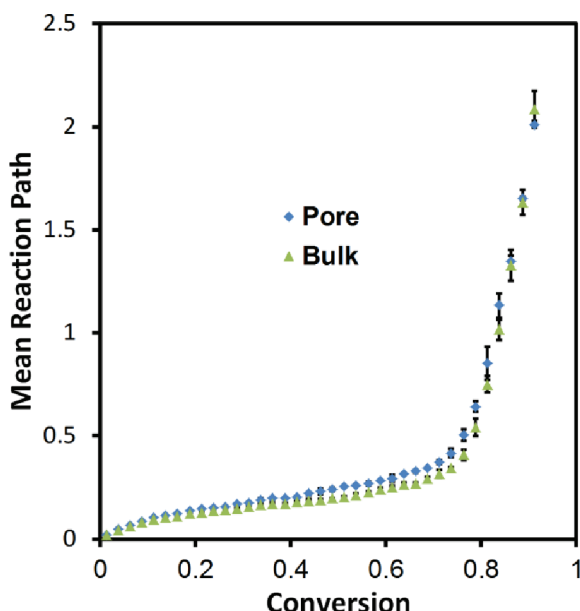


Figure 10. Conversion dependence of the mean reaction path in the bulk (green triangle) and the confined (blue diamond) systems for $P_0 = 10^{-3}$.

the total length of the actual traveled path) that a bead of epoxy monomers or cross-linkers undergoes from its initial position to the position where it reacts. Figure 10 shows a plot of the mean reaction path as a function of the conversion in the bulk and confined systems. We observed that up to 80% conversion, the mean reaction path of a bead in the confined system is more than that of a bead in the bulk system, suggesting that the reactants in the confined system have to diffuse through a longer distance to react. On the other hand, it was found that above 80% conversion, the mean reaction paths in the two systems do not show a measurable difference, with the values increasing steeply with conversion in both cases. We attribute this sharp rise in the mean reaction path to the low concentration of still-able-to-react beads at high conversion which necessitates longer diffusion of an epoxy monomer or a cross-linker before it reacts.

SUMMARY AND DISCUSSION

The nanoconfinement effect on the kinetics of cure reaction for cross-linked epoxy has been investigated in this study. We used a simple coarse-grained i.e., a dumbbell model to represent epoxy monomer and cross-linker. Reactive MD simulations were carried out to simulate the two-body and three-body autocatalytic reactions. In this simple model, epoxy monomer and cross-linker molecules react to form a new bond with a specified probability when both are in spatial proximity. The shape of the conversion curves obtained from our simulations is very similar to that obtained in the experiments.²¹ The kinetics of the reaction in the bulk was compared with that in a cylindrical pore. Our simulations show that over most of the conversion range, the overall translational mobility of still-able-to-react beads measured by mean-squared displacement is slightly higher in the confined system as compared to the bulk system, whereas the average required displacement of the beads from their initial position to the position of reaction is also slightly larger under the cylindrical confinement. The net result of these competing factors is that the

rate of curing reaction in the confined system is quantitatively similar to that in the bulk.

Even though the overall reaction rates in the confined system are almost the same as those in the bulk, we observed heterogeneity of the reaction rates in the confined system. As compared to the reaction rate in the bulk, the reaction rate in the first bead layer near the wall in the pore is consistently lower, while the reaction rate in the central core region of the pore is quantitatively similar to that in the bulk up to 70% conversion and becomes slightly higher in the high conversion stage. We attribute the low reaction rate in the first layer near the wall to the low translational mobility of the still-able-to-react beads in that layer as observed by mean-squared displacement (see Figure 8). This observation is in agreement with the literature observations that the mobility of the polymer chains is depressed near the physical constraints.^{7,16,17,31,32} Moreover, this heterogeneity of the reaction rates in the confined system suggests that the overall reaction rate in the confined systems will depend on the relative volume fractions of the outer shell domain (i.e., first layer near the wall) and the central core domain.

Previous lattice Monte Carlo (MC) simulation of stepwise polymerization has showed that the kinetics of polymerization could be accelerated in the highly confined systems in the absence of attractive interactions between both bonded and non-bonded sites.¹⁷ This effect was attributed to the packing of chains next to the pore walls. We note that for the lattice MC model used in that work, the system was highly ordered in nanoconfinement with the height of the first peak in the density distribution function being three to four times higher than the bulk value, whereas in our work, the height of the first peak near the wall is only about 50% higher than the bulk value (see Figure 4) and we did not find the kinetic enhancement of the curing reaction in this first bead layer. In addition, enhancement of the curing reaction rate of a cross-linked system has also been observed experimentally in the nanopore systems.^{8,9} Possible reasons for this discrepancy between these experiments and our simulations could be that the specific intermolecular interactions between the reactants as well as the effects of surface chemistry are not captured in our simple coarse-grained model. The model presented in this work captures the effect of diffusion on the rate of curing reaction in a nanopore. The model can be applied to study the effect of reaction gradient in confinement on the detailed topology of the network formed, and it can also be extended to incorporate the heat of reaction effects. These aspects will be topics for future work.

AUTHOR INFORMATION

Corresponding Author

*E-mail: rajesh.khare@ttu.edu.

Present Addresses

[†]Current address: Department of Chemical and Biological Engineering, University of Wisconsin—Madison, Madison, Wisconsin 53706, United States.

[‡]Current address: Department of Chemistry & Biochemistry, Texas Tech University, Lubbock, Texas 79409–1061.

ACKNOWLEDGMENT

The authors gratefully acknowledge the financial support received from National Science Foundation (NSF) under Grant

CMMI-0826437. The authors also thank Sindee Simon for insightful discussions.

■ REFERENCES

- (1) Jackson, C. L.; McKenna, G. B. *J. Chem. Phys.* **1990**, *93*, 9002–9011.
- (2) Jackson, C. L.; McKenna, G. B. *J. Non-Cryst. Solids* **1991**, *131*, 221–224.
- (3) Huck, W. T. S. *Chem. Commun.* **2005**, 4143–4148.
- (4) Alcoutlabi, M.; McKenna, G. B. *J. Phys.: Condens. Matter* **2005**, *17*, R461–R524.
- (5) Alba-Simionescu, C.; Coasne, B.; Dosseh, G.; Dudziak, G.; Gubbins, K. E.; Radhakrishnan, R.; Sliwinska-Bartkowiak, M. *J. Phys.: Condens. Matter* **2006**, *18*, R15–R68.
- (6) Varnik, F.; Binder, K. *Int. J. Mater. Res.* **2009**, *100*, 1494–1502.
- (7) Barrat, J. L.; Baschnagel, J.; Lyulin, A. *Soft Matter* **2010**, *6*, 3430–3446.
- (8) Li, Q. X.; Simon, S. L. *Macromolecules* **2008**, *41*, 1310–1317.
- (9) Li, Q. X.; Simon, S. L. *Macromolecules* **2009**, *42*, 3573–3579.
- (10) Koh, Y. P.; Li, Q. X.; Simon, S. L. *Thermochim. Acta* **2009**, *492*, 45–50.
- (11) Koh, Y. P.; Simon, S. L. *J. Phys. Chem. B* **2010**, *114*, 7727–7734.
- (12) Begum, F.; Simon, S. L. *Polymer* **2011**, *52*, 1539–1545.
- (13) Scheidler, P.; Kob, W.; Binder, K. *Europhys. Lett.* **2002**, *59*, 701–707.
- (14) Scheidler, P.; Kob, W.; Binder, K. *Eur. Phys. J. E* **2003**, *12*, 5–9.
- (15) Malvaldi, M.; Bruzzone, S.; Raos, G.; Allegra, G. *J. Phys. Chem. B* **2007**, *111*, 4141–4149.
- (16) Vogel, M. *Macromolecules* **2009**, *42*, 9498–9505.
- (17) Malvaldi, M.; Bruzzone, S.; Picchioni, F. *J. Phys. Chem. B* **2006**, *110*, 12281–12288.
- (18) Weeks, J. D.; Chandler, D.; Andersen, H. C. *J. Chem. Phys.* **1971**, *54*, S237–S247.
- (19) Khare, R.; de Pablo, J.; Yethiraj, A. *J. Chem. Phys.* **1997**, *107*, 2589–2596.
- (20) Pang, K. P.; Gillham, J. K. *J. Appl. Polym. Sci.* **1989**, *37*, 1969–1991.
- (21) Wisanrakkit, G.; Gillham, J. K. *J. Appl. Polym. Sci.* **1990**, *41*, 2885–2929.
- (22) Allen, M. P.; Tildesley, D. J. *Computer simulation of liquids*; Oxford University Press: New York, 1989.
- (23) Simon, S. L.; Gillham, J. K. *J. Appl. Polym. Sci.* **1992**, *46*, 1245–1270.
- (24) Tanaka, Y.; Bauer, R. S. Curing Reactions. In *Epoxy Resins: Chemistry and Technology*; May, C. A., Ed.; Marcel Dekker, Inc.: New York: 1988; p 298.
- (25) Xu, J.; Viasnoff, V.; Wirtz, D. *Rheol. Acta* **1998**, *37*, 387–398.
- (26) McKinley, S. A.; Yao, L.; Forest, M. G. *J. Rheol.* **2009**, *53*, 1487–1506.
- (27) Saxton, M. J. *Biophys. J.* **1994**, *66*, 394–401.
- (28) Condamin, S.; Tejedor, V.; Voituriez, R.; Benichou, O.; Klafter, J. *Proc. Natl. Acad. Sci. U.S.A.* **2008**, *105*, 5675–5680.
- (29) Szymanski, J.; Weiss, M. *Phys. Rev. Lett.* **2009**, *103*, 038102.
- (30) Skaug, M. J.; Faller, R.; Longo, M. L. *J. Chem. Phys.* **2011**, *134*, 215101.
- (31) Kusmin, A.; Gruener, S.; Henschel, A.; de Souza, N.; Allgaier, J.; Richter, D.; Huber, P. *Macromolecules* **2010**, *43*, 8162–8169.
- (32) Kusmin, A.; Gruener, S.; Henschel, A.; Holderer, O.; Allgaier, J.; Richter, D.; Huber, P. *J. Phys. Chem. Lett.* **2010**, *1*, 3116–3121.